

NO8600013

UNIVERSITY OF OSLO



INSTITUTE OF PHYSICS

REPORT SERIES

ON THE SPATIAL RELATIONSHIP BETWEEN AURORAL
EMISSIONS AND MAGNETIC SIGNATURES OF PLASMA
CONVECTION IN THE MIDDAY POLAR CUSP AND CAP
IONOSPHERES DURING NEGATIVE AND POSITIVE IMF B_z :
A CASE STUDY.

P.E. Sandholt, A. Egeland and B. Lybekk,
Institute of Physics, University of Oslo, Norway.

QUP --
Report 86-06 .

Received 6/3-1986

ABSTRACT. The dynamics of midday auroras, including polar cusp and cap emissions, and their relation to the interplanetary magnetic field (IMF) have been investigated with optical ground-based observations from Svalbard, Norway and IMF data from spacecraft ISEE-2. One case is presented, showing the spatial relationship - along the magnetic meridian in the midday sector - between the cusp aurora and IMF B_y -related convection currents (the DFY signature) for negative and positive values of IMF B_z .

INTRODUCTION.

A meridian chain of magnetometer stations rotating with the earth (Akasofu et al., 1983; Friis-Christensen et al., 1985; Friis-Christensen, 1985) may be used to obtain the average diurnal variation of equivalent currents over the northern hemisphere (Friis-Christensen and Wilhelm, 1975). The diurnal pattern of the IMF-related plasma convection in the polar ionosphere is then obtained by solving the differential equation relating the electric potential and the equivalent current function, derived from the ground-based measurements (cf. Kamide et al., 1981). Vennerström et al. (1984) studied the relationship between the latitudinal location of the DFY convection current and the F-region electron temperature enhancement usually associated with the cusp, measured by the Sonderstrom radar. In this report the relationship between the DFY signature and optical emissions in the polar cusp and cap is investigated for positive and negative values of IMF B_y .

OBSERVATIONS

Dayside auroral emissions were recorded by a set of meridian scanning photometers (MSPs) operated on Svalbard (Spitzbergen), an island group to the north of Norway. By this technique the dayside auroras can be observed within the range $\sim 70^\circ$ - 80° geomagnetic latitude at midwinter (cf. Sandholt et al., 1985). Local magnetic noon and solar noon at the recording site occurs at ~ 0830 and ~ 11 UT, respectively.

Geomagnetic disturbances were recorded by standard magnetometers at four stations on Svalbard, covering the range 71.1° -

75.4° geomagnetic latitude (cf. Table 1).

Between 06 and 08 UT on Jan. 04, 1984 the dayside aurora was located close to the southern boundary of the field of view of the photometer system in Longyearbyen, corresponding in time to a large negative IMF B_z component (cf. Fig. 1). In the period 0745-1000 UT three major changes in the IMF state took place. A strong disturbance was detected by the ISEE-2 spacecraft outside the bow-shock at \sim 0745 UT (cf. Fig. 1). The total field was suddenly enhanced by a factor of 3, from 10 to 30 nT, then decreasing after a few minutes to a stable level of \sim 20 nT. Associated with this change a switch of B_y from +7 to -17 nT occurred. B_x was changed from -10 to +3 nT, before returning to nearly the initial value. The three left panels in Fig. 1 show B_{total} , B_y , and B_z . These IMF traces have been shifted by approx. 15 minutes relative to the ground data, in order to take into account the time delay between the IMF signal detected by the satellite in the solar wind and the geophysical response observed on the ground.

A factor of 3 increase in the red oxygen emission at 630.0 nm occurred just before 08 UT, some 15 minutes after the IMF compression was detected outside the bow-shock. A subsequent decay of the red line started at 0800 UT and reached a stable level at 0815 UT. The blue band at 427.8 nm (N_2^+ 1. negative) did not show as large an initial enhancement as the red oxygen line. Zenith angle profiles obtained from the scanning photometer system are shown in Fig. 2. The red line intensity versus time and zenith angle is also presented in the middle panel of Fig. 1. The right panels show the H-component magnetic deflections at the stations Ny Alesund (NYA), Hornsund (HSD) and Bjørnøya (BJA). Notice the large negative disturbance between 0800 and 0840 UT at the southernmost station, located close to the latitude of the aurora.

The next major IMF transition occurred at 0818 UT, when B_z went positive. B_x changed from -6 to +3 nT at the same time. B_{total} and B_y did not change. After the B_z change the poleward boundary of the luminosity moved towards north. The H-component deflection also shifted northward, increasing at Hornsund and Ny Alesund, while decreasing at Bjørnøya. A rather narrow, east-west aligned discrete arc at the poleward boundary of the more diffuse red belt is a characteristic feature during this period (cf. Fig. 1, 0845 and 0900 UT panels). This arc is located close to the

minimum in the H-component deflection profile and the zero-point in the Z-component profile (cf. Fig. 3).

At ~ 0925 UT the IMF vector turned farther northward. This change was followed by a rapid poleward expansion in the equatorward boundary of the cusp aurora (cf. Fig. 1 middle panel and Fig. 2 last panel). From ~ 0900 UT auroral luminosity occurred near the southern edge of the field of view, separated from the aurora farther north and characterized by a relatively intense green oxygen line at 557.7 nm.

Figure 4 shows H-component magnetograms from 3 stations on the eastcoast of Greenland, ~ 2 hours to the west of Svalbard, i.e. in the pre-noon sector. Notice the anticorrelation in the deflection amplitude at Scoresbysund (SCO) and Danmarkshavn (DMH), when the IMF vector went from southward to northward orientation. A similar poleward expansion of the DPY signature is seen in the Svalbard records.

DISCUSSION

The observations presented above can be separated into three periods with different IMF orientation. These periods are indicated on Figure 1.

Period 1. The magnetic signature indicates a southwestward DPY current with the amplitude modulated by IMF B_z (B_y is constant near -17 nT). The local H-component perturbation at Hjørndøya shows only minor modulations correlated with the optical intensity. The observed DPY signature is interpreted as associated with the merging convection cell centered in the dawn sector of the polar ionosphere, with a northwestward flow (southeastward electric field) in the midday cusp region (cf. Heelis, 1984; Reiff and Burch, 1985; Banks et al., 1984).

Period 2. The transition in IMF B_z from negative to positive at 0818 UT (B_y not changing) was followed by marked changes in the optical aurora and the DPY signature. The location and motion of the aurora and the DPY perturbation are illustrated in Fig. 3. At 0900 UT the center of the westward DPY current is above the auroral observing site at Longyearbyen (ΔH max. negative and $\Delta Z = 0$). At this time the cusp aurora peaks in intensity somewhere to the south of the latitude of Hornsund. The

DPY equivalent current center is located at the poleward boundary of the cusp aurora. This shows that the DPY current extends into the polar cap from approximately the center of the optical cusp. This is in agreement with Vennerström et al. (1984), who found that the equatorward boundary of the DPY current is collocated with the latitude of maximum ionospheric electron temperature, usually associated with the center of the cusp region. The DPY current observed in time interval 2 is probably related to the polar cap lobe cell convection postulated for $B_z > 0$ (cf. Crooker, 1979; Reiff and Burch, 1985) and identified by use of the magnetometer chain along the westcoast of Greenland (Friis-Christensen, 1985a).

The discrete arc observed close to the poleward boundary of the optical cusp could be an effect of reconnection between the northward IMF and tail lobe field lines poleward of the cusp (e.g. Cowley, 1981).

The diffuse aurora observed to the south of Bjørndya from 09 UT onwards, with spectral characteristics indicating ~ 1 keV particle energy (cf. Figs. 1 and 2) is not associated with the cusp. One possible source is the dayside extension of the plasma sheet boundary layer (cf. also Makita et al., 1984).

Period 3. During this period, from 0940 to 1000 UT as observed from the ground, the IMF vector is pointing due north. This state should produce a net magnetic flux transfer from open lobe tubes to closed dayside tubes (cf. Cowley, 1981) with a resulting poleward motion of the equatorward boundary of the cusp. This expected effect is observed at 0940 UT. A weak cusp-like aurora is located to the north of Ny Alesund.

SUMMARY AND CONCLUSIONS

- i) The midday auroral luminosity often shows latitudinal differences in the spectral properties indicating different sources of the associated particle precipitation. Different particle source regions in the dayside magnetosphere, projecting to the ionosphere within the field of view of the scanning photometers at Svalbard are:

- a) The polar cap
- b) The polar cusp
- c) The dayside extension of the plasma-sheet boundary layer

The corresponding diversity of the dayside auroral emissions must be taken into account when discussing the cusp response to the IMF, based on optical data.

ii) The reported observations show that the IMF B_z component exert major influences on the latitudinal location and intensity of the polar cusp aurora. Concerning the possible influence from the magnetospheric substorm a reservation is expressed, due to lacking AE-index information at the time of publication.

iii) The changes in the DPY signatures which occurred when the IMF vector turned from southward to northward orientation are interpreted in terms of a disappearance of the merging cell convection in the midday cusp and at oval latitudes in the morning sector, simultaneously with an activation of the lobe cell convection farther north, within the polar cap (Friis-Christensen, 1985b).

The observed relationship between the latitudinal location of the cusp aurora and the DPY convection signature is:

a) IMF $B_z < 0$: The DPY signature maximizes at the latitude of the cusp aurora. This is consistent with existing models and observations of the merging cell, which convect magnetic flux from the closed dayside into the open polar cap, across the midday cusp. IMF $B_y < 0$ corresponds to southwestward DPY current (northeastward convection) in the cusp. The DPY amplitude is sensitive to IMF B_z variations.

b) IMF $B_z > 0$: The DPY signature of a westward current ($B_y < 0$), associated with the lobe cell convection, peaks at the poleward boundary of the red-dominated, diffuse cusp aurora. The cusp boundary and the DPY peak are collocated with a discrete arc showing a lower value of the spectral ratio $I(630.0\text{nm})/I(557.7\text{nm})$ (indicating higher energy particle precipitation), compared with the central cusp.

iv) During IMF $B_z < 0$ conditions the intensity of the cusp aurora was observed to be highly sensitive to solar wind

irregularities, indicating efficient plasma transfer. When IMF B_z turned due north the auroral intensity decreased towards a minimum, indicating reduced plasma transport into the magnetospheric cusp region.

ACKNOWLEDGEMENTS

It is a great pleasure to thank R.C. Elphic (University of California) for providing IMF data from satellite ISEE-2 (principal investigator: C.T. Russell) as well as S. Berger (University of Tromsø), and A.W. Wernik (Polish Academy of Sciences, Warszawa) for the ground magnetic recordings from stations on Svalbard. The Greenland magnetograms were kindly provided by E. Friis-Christensen (Danish Meteorological Institute).

REFERENCES

- Alasofu, S.-I., B.-H. Ahn, and G.J. Romick, A study of the polar current system using the IMS meridian chain of magnetometers. I. Alaska Meridian Chain, Space Sci. Rev., 36, 337, 1983.
- Banks, P.M., T. Araki, C.R. Clauer, J.P. St. Maurice, and J.G. Foster, The interplanetary electric field, cleft currents and plasma convection in the polar caps, Planet. Space Sci., 32, 1551, 1984.
- Cowley, S.W.H., Magnetospheric and ionospheric flow and the interplanetary magnetic field, in The Physical Basis of the Ionosphere in the Solar-Terrestrial System, Conf. Proc. AGARD-CP-295, p. 4-1, 1981, NATO, Neuilly-Sur-Seine.
- Crooker, N.U., Dayside merging and cusp geometry, J. Geophys. Res., 84, 951, 1979.
- Friis-Christensen, E., and J. Wilhjelm, Polar cap currents for different directions of the interplanetary magnetic field in the Y-Z plane, J. Geophys. Res., 80, 1248, 1975.
- Friis-Christensen, E., Solar wind control of the polar cusp, Danish Met. Inst., Geophysical Papers, R-72, 1985.
- Friis-Christensen, E., personal communication, 1985.
- Friis-Christensen, E., Y. Kamide, A.D. Richmond and S. Matsushita, Interplanetary magnetic field control of high latitude electric field and currents determined from Greenland magnetometer data. J. Geophys. Res., 90, 1325, 1985.
- Heelis, R.A., The effect of interplanetary magnetic field orientation on dayside high-latitude ionospheric convection, J. Geophys. Res., 89, 2873, 1984.
- Kamide, Y., A.D. Richmond, and S. Matsushita, Estimation of ionospheric electric fields, ionospheric currents, and field-aligned currents from ground magnetic records, J. Geophys. Res., 86, 801, 1981.
- Makita, K., C.-I. Meng, and S.-I. Akasofu, Temporal and spatial variations of the polar cap dimension and its relation to the energy input rate ϵ and AE index, J. Geophys. Res., 90, 2744, 1985.
- Reiff, P.H., and J.L. Burch, IMF B_y -dependent plasma flow and Birkeland currents in the dayside magnetosphere. 2. A global model for northward and southward IMF, J. Geophys. Res., 90, 1595, 1985.

Sandholt, P.E., A. Egeland, J.A. Holtet, B. Lybekk, K. Svenes, S. Asheim, and C.S. Deehr, Large- and small-scale dynamics of the polar cusp, J. Geophys. Res., 90, 4407, 1985.

Vennerstrøm, S., E. Friis-Christensen, T.S. Jørgensen, O. Rasmussen, C.R. Clauer, and V.B. Wickwar, Ionospheric currents and F-region plasma boundaries near the dayside cusp, Geophys. Res. Lett., 11, 903, 1984.

FIGURE CAPTIONS

Fig. 1: Left three panels: IMF measurements from the ISEE-2 satellite, i.e. total field, east-west (B_y) and north-south (B_z) components in the geocentric sun-ecliptic (GSE) coordinate system.

Middle panel: Intensity versus zenith angle and universal time of the red oxygen line at 630.0 nm, observed from Longyearbyen (74.4° geom.lat.).

Right three panels: H-component magnetic disturbance detected at the three stations Ny Alesund (NYA), Hornsund (HSD), and Bjørnøya (BJA). Negative deflection towards left. The data recorded on the ground have been shifted by ~ 15 min. relative to the IMF traces.

Fig. 2: North-south magnetic meridian scan profiles for the three wavelengths 630.0 nm (OI), 427.8 nm (N_2^+), and 557.7 nm (OI) observed at five selected times during the period shown in Fig. 1. Intensity scales are marked to the left.

Fig. 3: Latitude profiles of the Z- and H-components of the magnetic disturbance, based on recordings from the four Svalbard stations located as shown on the horizontal axis. The scale on the vertical axis is in nanoteslas. The latitudinal location of auroral luminosity is estimated from the photometer profiles in Fig. 2.

Fig. 4: H-component magnetograms (negative deflection downwards) from three stations on the eastcoast of Greenland, Danmarkshavn (DMH), Daneborg (DNB), and Scoresby-sund (SCO). The time intervals corresponding to different IMF B_z polarities (B_y nearly constant) are indicated. The time delay from the satellite to the ground has been taken into account.

TABLE 1. LIST OF GEOMAGNETIC OBSERVATORIES ON SVALBARD

Station name	Station code	Geographic		Geomagnetic		Computed magnetic dip angle	L-value
		Lat.	Long. (East)	Lat.	Long.		
Ny Alesund	NYA	79.00	12.00	75.44	131.45	81.5	16.5
Longyearbyen	LYR	78.20	15.70	74.36	130.94		14.4
Hornsund	HSD	77.0	15.6	73.54	127.77	81.3	13.1
Bjørnøya	BJA	74.50	19.20	71.08	124.55	79.6	9.5

JAN. 1984

INTERPLANETARY MAGNETIC FIELD
(nanoteslas)

CUSP AURORA
SVALBARD
(630.0nm)

H-COMP MAGNETOGRAMS
SVALBARD

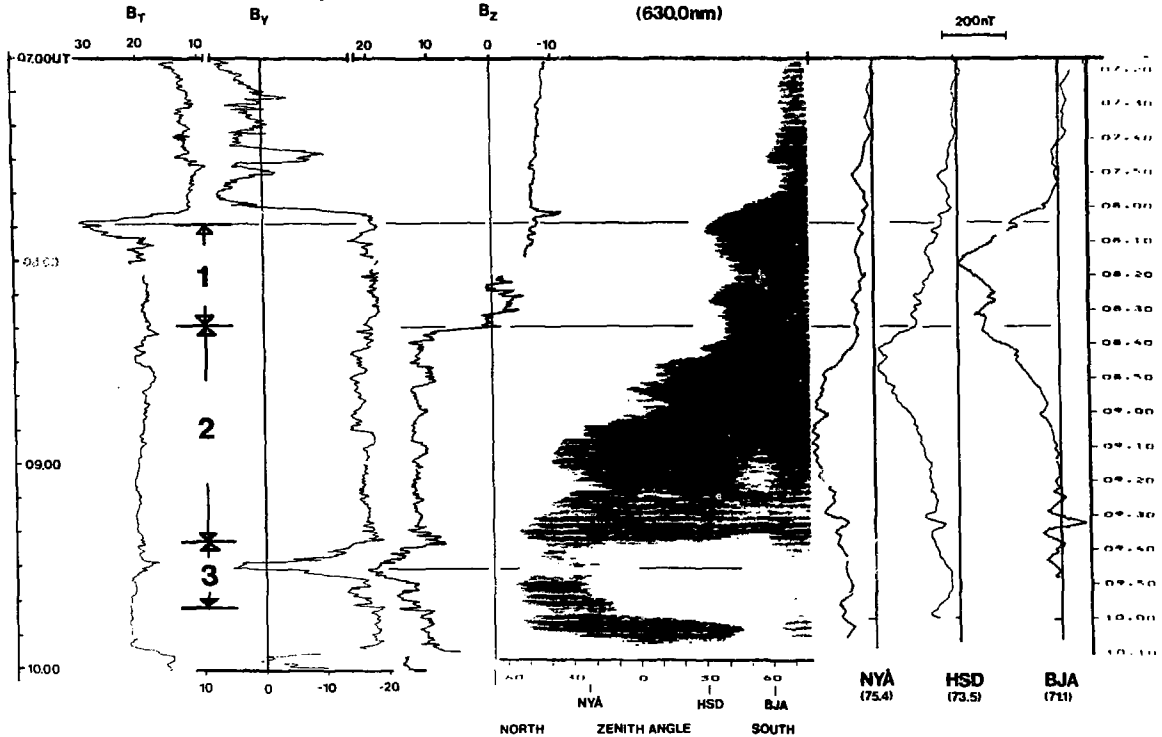


FIG. 1

**MIDDAY AURORA
SVALBARD
JAN.04,1984**

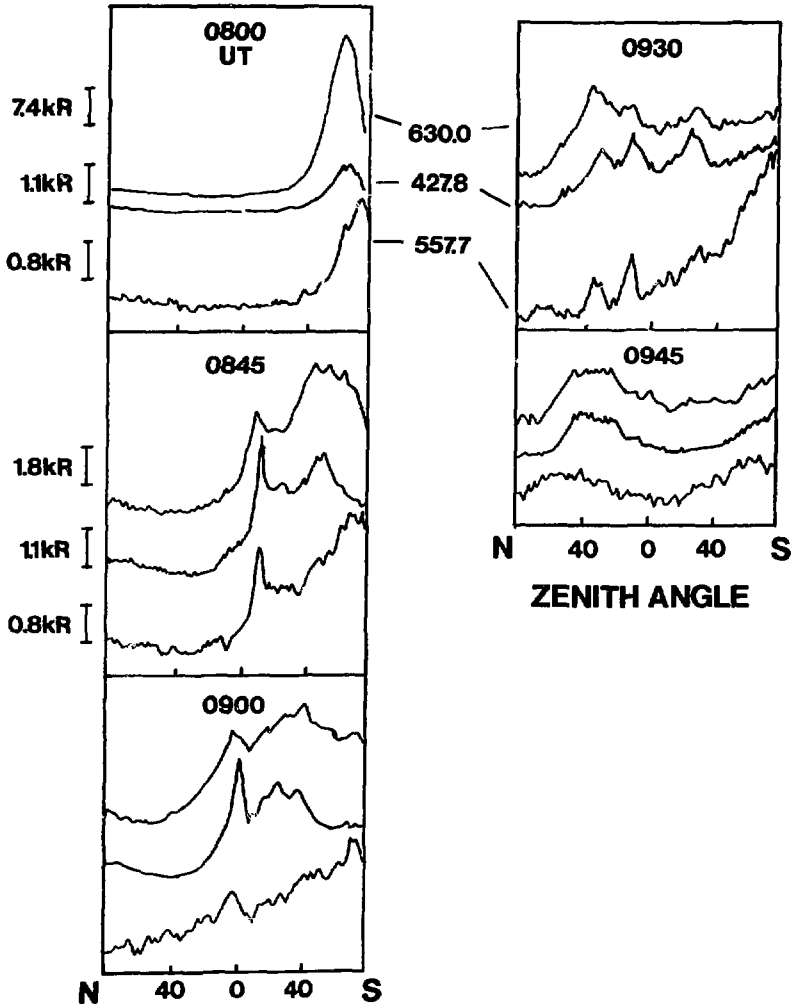


FIG.2

**SVALBARD
JAN.04,1984**

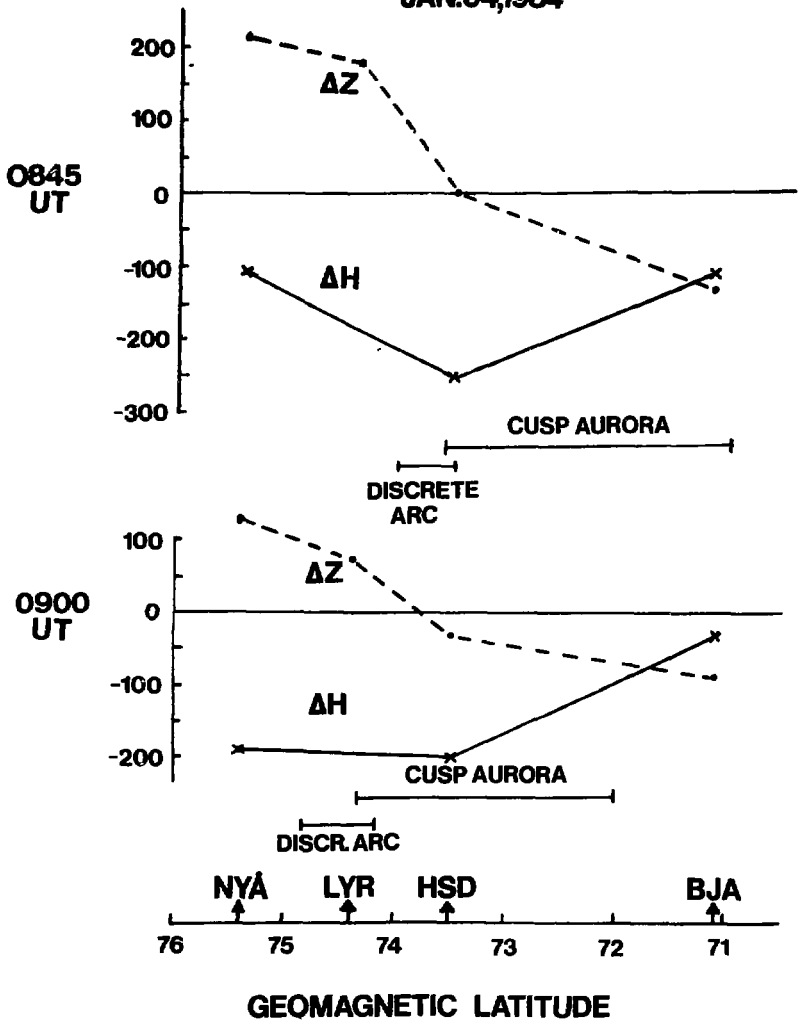


FIG.3

GREENLAND JAN. 04, 1984
H-COMP MAGNETOGRAMS

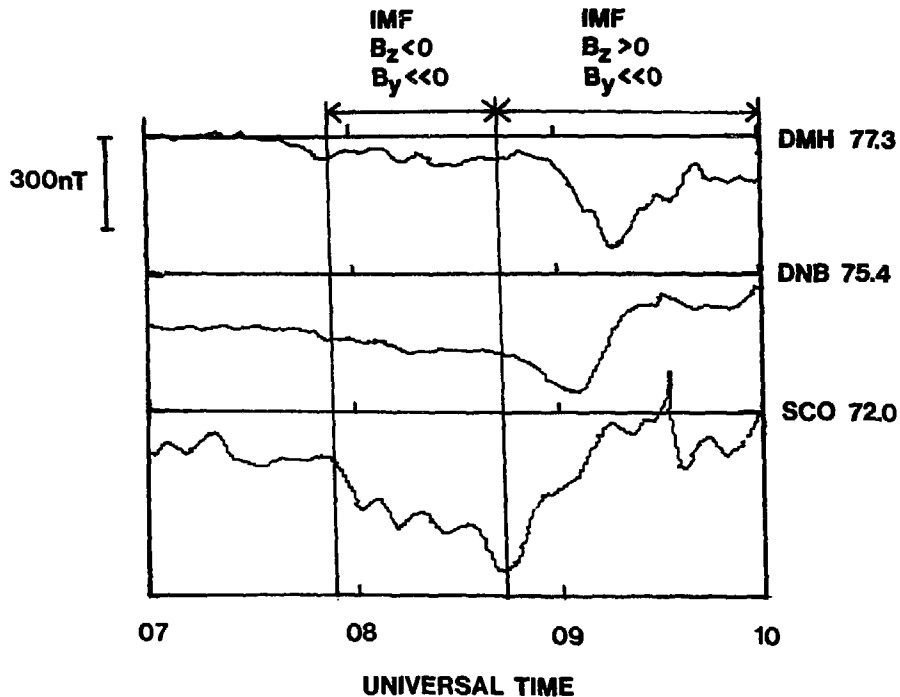


FIG.4